Catalysis Today 146 (2009) 336–344

Contents lists available at ScienceDirect

Catalysis Today

journal homepage: www.elsevier.com/locate/cattod

Electrochemical promotion of the CO_2 hydrogenation reaction using thin Rh, Pt and Cu films in a monolithic reactor at atmospheric pressure

E.I. Papaioannou, S. Souentie, A. Hammad, C.G. Vayenas *

Laboratory of Chemical and Electrochemical Processes (LCEP), Department of Chemical Engineering, University of Patras, Caratheodory 1 Street, GR-26504, Patras, Greece

ARTICLE INFO

Article history:
Available online 23 July 2009

Keywords:
CO_2 hydrogenation
NEMCA effect
EPOC
Rh electrodes
Pt electrodes
Cu electrodes

ABSTRACT

A monolithic electropromoted reactor (MEPR) with up to 22 thin Rh/YSZ/Pt or Cu/TiO_2/YSZ/Au plate cells was used to investigate the hydrogenation of CO_2 at atmospheric pressure and temperatures 220–380 °C. The Rh/YSZ/Pt cells lead to CO and CH_4 formation and the open-circuit selectivity to CH_4 is less than 5%. Both positive and negative applied potentials enhance significantly the total hydrogenation rate but the selectivity to CH_4 remains below 12%. The Cu/TiO_2/YSZ/Au cells produce CO, CH_4 and C_2H_4 with selectivities to CH_4 and C_2H_4 up to 80% and 2%. Both positive and negative applied potential significantly enhance the hydrogenation rate and the selectivity to C_2H_4. It was found that the addition of small (~0.5 kPa) amounts of CH_3OH in the feed has a pronounced promotional effect on the reaction rate and selectivity of the Cu/TiO_2/YSZ/Au cells. The selective reduction of CO_2 to CH_4 starts at 220 °C (vs 320 °C in absence of CH_3OH) with near 100% CH_4 selectivity at open-circuit and under polarization conditions at temperatures 220–380 °C. The results show the possibility of direct CO_2 conversion to useful products in a MEPR via electrochemical promotion at atmospheric pressure.

1. Introduction

In recent years the hydrogenation of CO_2 to hydrocarbons has received worldwide attention both as a potential source of renewable fuels and as a potential means of decreasing the overall CO_2 emissions.

Due to the use of Cu–ZnO/Al_2O_3 catalysts in the industrial process of methanol synthesis at temperatures 220–300 °C and pressure from 50 to 100 atm, Cu and Rh based catalysts have been also studied for CO_2 reduction to hydrocarbons [1–29].

Most studies of the catalytic hydrogenation of CO_2 have been performed in fixed-bed reactors using mainly metal catalysts (e.g. Rh, Pd, Ru, Cu, Fe, Co, Ni) supported over several metal oxide supports (e.g. Nb_2O_3, ZrO_2, Al_2O_3, SiO_2) [1–37] and utilizing high pressures (5–70 atm) [5–9,20–26,28], which increase the thermodynamic equilibrium conversion to methanol and to light hydrocarbons. The products obtained in these studies utilizing Rh or Cu catalysts are presented in Table 1.

The nature of the intermediate compound involved in the rate-determining step of the process and on the methane formation scheme is still under discussion. It is not clear whether methane forms via the produced CO or whether CO_2 immediately converts into CH_4. Some research groups [30–32,38] believe that, after the dissociative adsorption of CO_2 yielding CO on the catalyst surface, the reaction follows the same mechanism as CO methanation. Another point of view was taken in [3,13,33]; in these studies, it was shown that CO does not participate in the carbon dioxide methanation reaction, i.e. the mechanisms of hydrogenation of CO and CO_2 are different. It is believed that the slow reaction step is either the formation of an intermediate CH_xO species and its interaction with hydrogen [14,37] or the formation of surface carbon from CO dissociation and its hydrogenation [16,34,36]. Weatherbee and Bartholomew [32] have shown that power equations cannot adequately describe the process and that the Langmuir–Hinshelwood equation better fits the experimental data.

When co-feeding CO_2 and H_2 over a hydrogenation catalyst, as in the present case, there are two main processes which can take place, i.e.:

$$CO_2 + H_2 \rightarrow CO + H_2 \quad (1)$$

$$xCO_2 + (2x - z + y/2)H_2 \rightarrow C_xH_yO_z + (2x - z)H_2O \quad (2)$$

The former is the reverse water–gas shift reaction (RWGS), which is a redox reaction, the latter is a synthesis reaction leading to the formation of hydrocarbons or (and) alcohols. Thus for $x = 1$, $y = 4$ and $z = 0$ one has the methanation reaction and for $x = 1$, $y = 4$ and $z = 1$ one has the methanol synthesis reaction.

The goal of the present investigation was to study the effect of catalyst potential and concomitant addition or removal of O^{2-} to or from the catalyst, which is in contact with Yttria-stabilized-Zirconia

* Corresponding author.
E-mail address: cat@chemeng.upatras.gr (C.G. Vayenas).

0920-5861/$ – see front matter © 2009 Elsevier B.V. All rights reserved.
doi:10.1016/j.cattod.2009.06.008

Table 1
Studies of the carbon dioxide hydrogenation reaction using several catalysts.

Catalyst	Experimental conditions	Products	Reference
Cu (polycrystal) Cu (1 1 1)	Aqueous, 0.1 M $KHCO_3$	CH_4, C_2H_4, CO	[27]
CuO/ZrO_2	$4H_2$:$1CO_2$, 50 atm, 220–280 °C	CH_3OH, CO, H_2O, CH_4	[7]
CuO/Al_2O_3			
CuO/TiO_3			
$CuO/ZrO_2/Al_2O_3$			
$CuO/ZrO_2/CeO_3$			
$CuO/ZrO_2/SiO_2$			
CuO/ZrO_2	$3H_2$:$1CO_2$, 15 atm, 400–600 °C	CH_3OH, CO	[6]
Cu–Fe	$4H_2$:$1CO_2$, 50 atm, 400 °C	CO, olefins C_n (n = 1–3)	[28]
Cu–Fe–Na			
$PdO/CuO/ZnO/Al_2O_3$	$4H_2$:$1CO_2$, 50 atm, 250 °C	CH_3OH, CO, H_2O	[8]
Rh/Nb_2O_5	$4H_2$:$1CO_2$, 1 atm, 250–350 °C	C_2–HC	[1]
Cu/SiO_2–Rh/Nb_2O_5			
Rh–YSZ	Various P_{CO_2}, P_{H_2}, 1 atm, 328–477 °C	CO, CH_4	[29]
Rh/Al_2O_3	$4H_2$:$1CO_2$, 1 atm, 170–200 °C	CH_4, CO	[2]
Rh/TiO_2			
Rh/SiO_2			
Pt–Ca/C	$3H_2$:$1CO_2$, 1–20 atm, 200–300 °C	CO, CH_4	[10]
Pt/SiO_2	$6H_2$:$3CO_2$, 50 atm, 250 °C	CO	[9]

(YSZ) an O^{2-} conductor, on the rates of reactions (1) and (2) and on the product selectivity to hydrocarbons.

The electrochemical promotion of catalysis (EPOC or NEMCA effect) has been investigated for more than 70 different catalytic systems using a variety of metal catalysts (or conductive metal oxides), solid electrolytes and catalytic reactions [39–52]. Work in this area has been reviewed recently [40]. In electrochemical promotion studies the conductive catalyst is in contact with an ionic conductor and is electrochemically promoted by applying a current or potential between the catalyst film and a counter electrode. As shown by numerous surface science and electrochemical techniques, including STM [41], electropromotion is due to electrochemically controlled migration (reversible backspillover or spillover) of promoting or poisoning ionic species (O^{2-} in the case of YSZ, TiO_2 and CeO_2, Na^+ in the case of β''-Al_2O_3, protons in the case of Nafion) between the ionic or mixed ionic-electronic conductor and the gas-exposed catalyst surface through the catalyst–gas–solid electrolyte three phase boundaries (tpb).

There have been two previous studies of the electrochemical promotion of CO_2 hydrogenation using YSZ solid electrolyte [53,54] and utilizing Rh [53] and Pd [54] catalyst-electrodes in a single chamber reactor. In the latter study, which was limited to temperatures above 530 °C, only CO was produced [54]. In the case of Rh catalyst films [53] CO and CH_4 were produced at temperatures 346–477 °C. It was found that the rate of CH_4 formation is enhanced with positive potentials (electrophobic behavior) and the rate of CO formation is enhanced with negative potentials (electrophilic behavior) with ρ values up to 3.7 and 2.7, respectively. The maximum selectivity to CH_4 was 35% [53].

Two parameters are commonly used to quantify the magnitude of electrochemical promotion effect:

1. the rate enhancement ratio, ρ, defined from:

$$\rho = \frac{r}{r_o} \tag{3}$$

where r is the electropromoted catalytic rate and r_o the normal, i.e. open-circuit catalytic rate.

2. the apparent Faradaic efficiency, Λ, defined from:

$$\Lambda_i = \frac{\Delta r_{catalytic}(\text{g-eq/s})}{(I/F)} \tag{4}$$

where $\Delta r_{catalytic}$ is the current- or potential-induced change in catalytic rate (g-eq/s), I the applied current and F the Faraday's constant. In this study where CH_4, CO and C_2H_4 are produced through the hydrogenation of CO_2, the Faradaic efficiency for each product formation is defined from:

$$\Lambda_{CO} = \frac{2\Delta r_{CO}(\text{mol/s})}{(I/F)}; \quad \Lambda_{CH_4} = \frac{8\Delta r_{CH_4}(\text{mol/s})}{(I/F)};$$
$$\Lambda_{C_2H_4} = \frac{6\Delta r_{C_2H_4}(\text{mol/s})}{(I/F)} \tag{5}$$

A reaction is termed electrophobic when its rate increases with positive current or potential and electrophilic when the rate increases with negative current or decreasing potential [41]. In the case of oxidation reactions on catalysts deposited on O^{2-} conductors, such as YSZ, a distinctive feature of electrochemical promotion is that $|\Lambda| > 1$. However, in the present case of reactions (1) and (2), since O_2 is not a reactant any positive current or positive potential-induced catalytic rate change is electrochemical promotion even when $|\Lambda| < 1$. This is not at first very clear in the case of negative current since it might be argued that CO_2 is decomposed to CO via O^{2-} abstraction, but negative current, i.e. O^{2-} removal from the catalyst, cannot lead to H_2O formation, thus again any current or potential-induced change in catalytic rate is electrochemical promotion.

A monolithic electrochemically promoted reactor, which has been described previously [55,56], was used in the present study equipped with Yttria-stabilized-Zirconia solid electrolyte plates, on which two catalytic electrodes were deposited. Two different electrocatalytic cell types have been used (a) Rh/YSZ/Pt elements and (b) Cu/TiO_2/YSZ/Au elements. The reactor operation pressure was constant at 1 atm. The CO_2 partial pressure in the feed was 1–1.1 kPa during all the experiments while the H_2 partial pressure was varied between 3 and 10 kPa although all results presented here were obtained with $P_{H_2} = 5.6$ kPa. The total gas flow rate was 1000 cm^3/min, unless stated otherwise.

2. Experimental

2.1. YSZ solid electrolyte plates

The solid electrolyte plates provided by Bosch had a thickness of 0.25 mm and dimensions of 50 mm × 50 mm. They were made of Yttria-stabilized-Zirconia (8 wt.% Y_2O_3 with a resulting molar composition $Zr_{0.913}Y_{0.087}O_{1.957}$). The starting material had a mean particle size of 0.5 μm. The density in the sintered state was between 5.7 and 5.9 g/cm^3.

2.2. Catalyst preparation

2.2.1. Rh/YSZ/Pt and Pt/YSZ/Au

The 22 Rh/YSZ/Pt type samples were prepared by metal sputtering. Prior to Rh or Pt deposition, no surface treatment was performed. The YSZ support was introduced into the sputtering chamber, filled with pure argon, then metal (Rh 99.8% or Pt 99.99%, Lesker) was deposited onto the substrate at 50 °C. The sputtering conditions were the following: direct current (dc) mode with a discharge of 350 V, argon pressure of 0.5 Pa. Under these conditions the deposition rate is 0.10–0.15 nm/s. The film thickness was measured by calibration with smooth silicon samples processed simultaneously. The thickness of the sputter-deposited rhodium and platinum films was 40 nm.

Also, in a effort to separate the catalytic and EPOC behavior of Rh and Pt catalyst-electrodes, 4 Pt/YSZ/Au electrocatalytic cells were prepared. The Pt film was also deposited by metal sputtering while the Au counter electrode was prepared by application of metalorganic paste (Metalor, Gold resinate, A1118) followed by drying at 400 °C for 90 min and calcination at 650 °C for 30 min.

2.2.2. Cu/TiO_2/YSZ/Au

Preliminary experiments with Cu sputtered films directed deposited on YSZ showed low catalytic activity, very low currents, practically no electrochemical promotion and very poor catalyst adhesion and lifetime. It was thus decided to first deposit a thin TiO_2 film on the YSZ and then to deposit the Cu catalyst on the TiO_2 layer. This approach, first introduced by the group of Comninellis [57] for Rh films has been shown to lead to very good electropromotion performance [57,58]. It should be noted that TiO_2 alone can lead to pronounced electrochemical promotion behavior of oxidation reactions [59] since under oxidizing conditions up to 3% of the current is ionic (O^{2-}) and the remaining 97% is electronic [59]. Under the reducing conditions of the present investigation, where the conductivity is entirely electronic [59] the beneficial role of TiO_2 is not obvious but must stem from the enhanced electronic conductivity of the film even under conditions (anodic polarization) where Cu will otherwise tend to be oxidized, and by the enhanced adhesion of the Cu film on the TiO_2 surface.

The 20 Cu/TiO_2/YSZ/Au type electrocatalytic cells were also prepared by metal sputtering. Initially a thin (~90 nm) TiO_2 film was sputter-deposited on the one side of the YSZ plate and then, additionally, a second thicker (~400 nm) layer of Cu was deposited over the TiO_2 thin film. For the above films a magnetron sputtering system was used. High purity argon and oxygen have been used as sputtering and reactive gas, respectively. The discharge characteristics have been controlled using a variable dc power supply (1 kV and 2 A). Pure titanium (99.95%) and copper (99.95%) have been used as sputtering targets.

Titania films were prepared on the YSZ substrates with 600 W target power, which enables 0.5 nm/min deposition rate and leads to a ca. 90 nm thickness film after 3 h of deposition. The substrate temperature was stable during the deposition at 250 °C. Also, a post-deposition annealing of the deposited TiO_2 film was performed in air at 600 °C for 60 min. Copper was deposited on TiO_2/YSZ substrates holding the target power stable at 280 W, which enables a 20 nm/min deposition rate, achieving a 400 nm thickness Cu film after 20 min of deposition. The substrate temperature was kept stable at 50 °C. For all the depositions the substrates were placed 55 cm far from the target which was found to result in good uniformity of the produced films. Fig. 1 presents a SEM micrograph of the Cu/TiO_2/YSZ surface.

The Au counter electrodes were prepared by application of metalorganic paste (Metalor, Gold resinate, A1118) followed by drying at 400 °C for 90 min and calcination at 650 °C for 30 min. Blank experiments using Au/TiO_2/YSZ/Au elements showed that the Au electrodes were practically catalytically inactive for the CO_2 hydrogenation reaction, establishing that the observed rate values correspond only to the rate on the Cu catalyst-electrode.

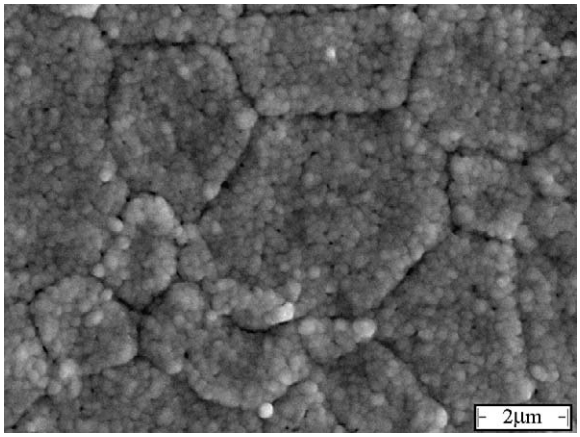

Fig. 1. SEM image of the Cu/TiO_2/YSZ surface.

2.3. Catalyst-electrode characterization

The surface area of the Rh, Pt and Cu catalytic films, as well as the metal dispersion, was estimated using the galvanostatic transient technique, by measuring the time constant, τ, required for the rate increase, Δr, in galvanostatic electropromotion rate transients to reach 63% of its steady state value [41]. In this way one can estimate the reactive oxygen uptake, N_G, of the anodically polarized metal film and, assuming a 1:1 surface metal:O ratio, the active catalyst surface area, N_G, expressed in mol, is calculated by:

$$N_G = I\tau/(2F) \quad (6)$$

during the current imposition [41] or by:

$$N_G = r\tau_D/\Lambda \quad (7)$$

in the current interruption technique [41], where r is the electropromoted rate and the depolarization time, τ_D, expresses the average lifetime of the backspillover oxygen species originating from the YSZ lattice. These promoting $O^{\delta-}$ species are more strongly bonded to the catalytic surface than normally adsorbed oxygen [41].

For the 22 Rh/YSZ/Pt elements these experiments were conducted both with anodic and cathodic polarization galvanostatic transients in an effort to estimate the surface area of both the Rh and Pt catalysts.

The total surface area of the Rh catalysts per plate was estimated to be $(1.0–6.0) \times 10^{-6}$ mol Rh and $(2.0–4.0) \times 10^{-6}$ mol Pt, close to those estimated in [55,56]. Since the metal loading per plate is of the order of 10^{-5} mol Rh or Pt, it follows that these thin (~40 nm) films are porous and mostly amorphous and that the Rh and Pt metal dispersions are of the order of 10–40%, i.e. comparable to that of commercial dispersed catalysts.

It should be noted that, in the present study, both the Rh and Pt films are catalytically active and therefore the measured consumption rate of CO_2 values correspond to the sum of the rates on the Rh and Pt catalyst films. Therefore the terms "electrophobic" ($dr/dU > 0$), "electrophilic" ($dr/dU < 0$), "volcano" and "inverted volcano" used to describe the observed electropromotion behavior are used in broad sense, characterizing the electropromotion behavior of the Rh/YSZ/Pt elements (U is the potential of the Rh catalyst-electrode relative to the Pt electrode) rather than that of the individual Rh and Pt catalysts.

For the 20 Cu/TiO_2/YSZ/Au elements, the total surface area of the Cu catalyst per plate was estimated to be $(5.0–9.0) \times 10^{-5}$ mol

Cu (by anodic polarization galvanostatic transient), almost one order of magnitude larger than the corresponding value for the Rh/YSZ/Pt elements. Since the metal loading per plate is of the order of 5×10^{-5} mol Cu, it follows, similar to the Rh and Pt films, that these thick (~400 nm) films are also porous and that again the metal (Cu) dispersion is of the order of 10–30%, i.e. comparable to that of commercial dispersed catalysts.

2.4. MEP reactor operation

The monolithic electrochemically promoted reactor was placed in a tubular furnace and its temperature was measured and controlled by a type K thermocouple at a distance of 1 mm from the gas entrance. The feed gas composition and total flow rate, F_T, was controlled by four mass flowmeters (Brooks smart mass flow and controller, B5878). Reactants were Messer–Griesheim certified standards of CO_2 in He and H_2 in He. Pure He (99.99%) was fed through the fourth flowmeter in order to further adjust total flow rate and inlet gas composition at desired levels. CO_2 and H_2 pressure was held constant at 1 and 5.6 kPa, respectively. The total gas flow rate was 1000 cm^3/min while the total pressure was constant at atmospheric. Reactants and products were analyzed by on-line gas chromatography (Varian 3800, equipped with a Porapaq-QS column at 50 °C for the separation of the produced C_xH_y and at 100 °C for the separation of CH_3OH), in conjunction with an IR CO_2–CO analyzer (Fuji Electric). Constant currents and potentials were applied using an AMEL 2053 galvanostat–potentiostat.

3. Results and discussion

3.1. CO_2 hydrogenation over 22 Rh/YSZ/Pt cells

Utilizing the 22 Rh/YSZ/Pt cells, only CH_4 and CO were formed at open-circuit and under anodic and cathodic polarization conditions.

Fig. 2 shows the steady state effect of temperature on the CO_2 reduction rate and conversion and on the selectivity to CH_4 under open-circuit and anodic (+3 V) and cathodic (−3 V) polarization conditions at temperatures from 280 to 380 °C and total gas flow rate 1000 cm^3/min. The open-circuit state CO_2 conversion increases from 0.1% at 280 °C to 2.5% at 380 °C, while CH_4 production occurs only at high temperatures (>360 °C) with corresponding selectivity ~5%. Anodic or cathodic polarization leads to significant increase in the CO_2 conversion with ρ values up to 4.7. The CH_4 selectivity also increases significantly. Thus CH_4 production starts already at 280 °C and at 300 °C reaches values of 13% and 12% under positive and negative polarization, respectively.

We have also found from Arrhenius plots of the open-circuit and electropromoted rates that significant variations occur in activation energies with potential as in many electropromotion studies [41]. Thus the activation energy for CO production decreases from ~17 kcal/mol under open-circuit to 13 and 11 kcal/mol, respectively, for anodic (+3 V) and cathodic (−3 V) polarization. The CH_4 formation activation energy is 21 kcal/mol under anodic polarization (+3 V) and 19 kcal/mol under cathodic polarization (−3 V). Thus the selectivity to CH_4 increases with temperature as shown in Fig. 2.

Fig. 3 shows the steady state effect of the applied potential on the rates of the CO_2 reduction and CO and CH_4 production at 320 °C (top) and 380 °C (bottom). An apparent "inverted volcano" type behavior of both reactions, i.e. both the CO and CH_4 rates increase both with anodic and with cathodic polarization. The corresponding effect of applied potential on the CO_2 conversion and the selectivity to CH_4 is shown in Fig. 4. As already discussed, it is noteworthy that at lower temperatures (e.g. 320 °C) the open-circuit selectivity to CH_4 is zero.

In an effort to rationalize the observed apparent inverted volcano behavior and to separate the role of Rh and Pt in the monolithic electropromoted reactor (MEPR) environment, we have used in a separate set of experiments four Pt/YSZ/Au type cells. The results are presented in Fig. 5, and show the steady state effect of the applied potential on the CO_2 reduction and CO formation catalytic rates and on the CO_2 conversion at 380 °C. As shown, in Fig. 5 over Pt only CO has been detected in the products, demonstrating an inverted volcano type behavior [41]. Accounting for the observed high selectivity to CO of the Pt catalyst-electrode, we can conclude that on the Rh surface both CH_4 and CO are

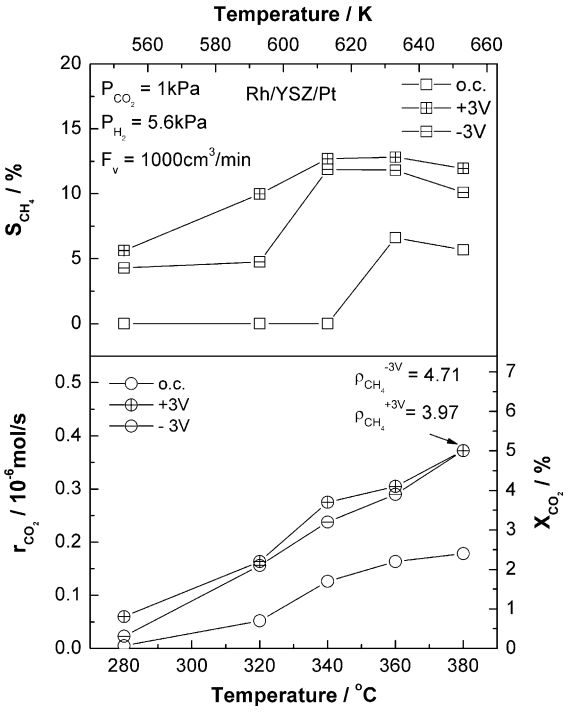

Fig. 2. Effect of temperature on the CO_2 reduction rate, on the CO_2 conversion and on the selectivity to CH_4 under open-circuit and anodic (+3 V) and cathodic (−3 V) polarization conditions utilizing 22 Rh/YSZ/Pt cells.

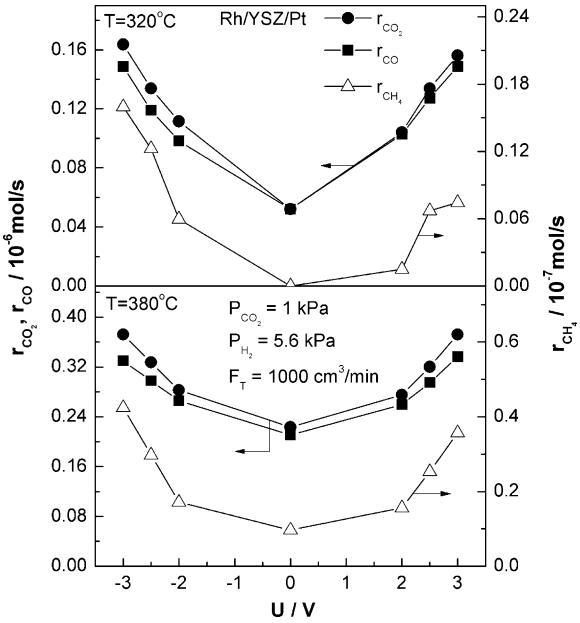

Fig. 3. Effect of applied potential on the CO_2 reduction rate and on the CO and CH_4 formation catalytic rates at 320 °C (top) and 380 °C (bottom) utilizing 22 Rh/YSZ/Pt cells.

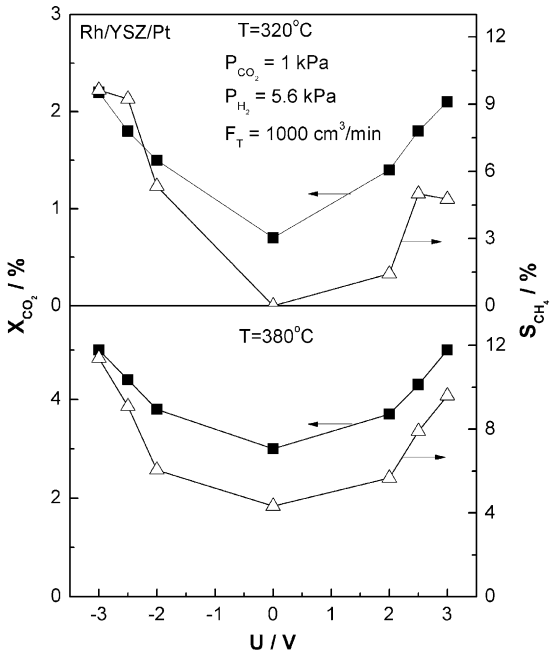

Fig. 4. Effect of applied potential on the CO_2 conversion and on the selectivity to CH_4 at 320 °C (top) and 380 °C (bottom) utilizing 22 Rh/YSZ/Pt cells.

formed while on Pt only CO is produced, in agreement with several previous studies [9,38,44]. Hence, the apparent inverted volcano type behavior of the methanation reaction is characteristic of Rh and can be attributed to the low coverages of both CO_2 and dissociatively adsorbed H at the high operating temperatures and low CO_2 and H_2 partial pressures of the present investigation [41] and thus to the increase of hydrogen (electron donor) and CO_2 (electron acceptor) coverage of the catalytic surface (Rh) upon positive and negative polarization respectively, as expected from the electrochemical promotion rules [41].

As discussed above, the observed inverted volcano type behavior of the CH_4 formation reaction on Rh films, can be attributed to the increase of the hydrogen adsorption strength upon anodic potential application while the increase of the rates of CO formation, from the dissociation of CO_2 upon cathodic polarization. Negative potential application causes an increase in the adsorption bond strength of CO, which acts as an electron acceptor. This enhances the dissociation of the adsorbed CO species leading to formation of organic products. This step, i.e. the dissociation of the adsorbed CO seems to be the rate limiting step according to several studies [2,11,19]. On the other hand positive polarization seems to be more complex, but is similar to what Zhang et al. [12] have proposed utilizing a W^{6+} doped Rh/TiO_2 dispersed catalyst. They propose an increase of the adsorption bond strength of H due to the W^{6+} doping, which favors the formation of Rh carbonyl hydride species. These species consist of a Rh carbonyl complex and one or two hydrogen atoms associated to CO via the Rh center:

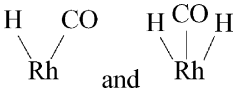

Due to charge transfer from the bonded H to the Rh center, the π-donation from Rh into an anti-bonding π-orbital of CO is enhanced. Consequently, the C–O bond is significantly weakened whereas the Rh–CO bond is strengthened (backdonation) [12]. Thus the dissociation of CO is much easier than without doping. This doping process in classical promotion is similar to the positive polarization in EPOC studies. Positive polarization, i.e. O^{2-} supply form the Pt counter electrode to the Rh catalytic surface, enhances the adsorption bond strength of H (electron donor), leading in a similar way to the formation of Rh carbonyl hydride species, due to electronic promotion by the co-adsorbed H species.

The effect of gas flow rate at constant feed composition on the CO_2 reduction and CH_4 formation catalytic rates, on the CO_2 conversion and on the selectivity to CH_4 under open-circuit and imposed potential conditions, is shown in Fig. 6. The CO_2 reduction and CH_4 formation rates under polarization conditions initially increase with flow rate increase reaching a plateau at high flow rates ($\geq$1000 cm^3/min), while CO_2 conversion decreases continuously from 10% to 2% under negative potential application and from 5% to 1% under open-circuit conditions. This indicates the absence of any mass transfer limitation phenomena. On the other hand, the CH_4 selectivity under open-circuit conditions remains stable at 5%, while upon positive (+3 V) and negative (−3 V) polarization it is constant at 10% and 13%, respectively. This shows that both CH_4 and CO are produced in parallel routes from reactions (1) and (2), since a decrease in selectivity to CH_4 with flowrate would be expected if CH_4 were produced from CO in a consecutive step.

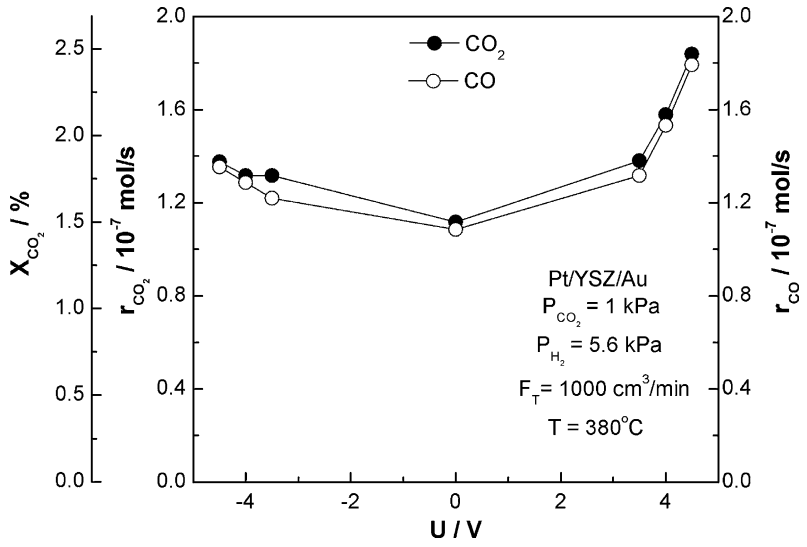

Fig. 5. Effect of the applied potential on the CO_2 reduction rate, on the conversion of CO_2 and on the CO production rate at T = 380 °C utilizing 4 Pt/YSZ/Au cells.

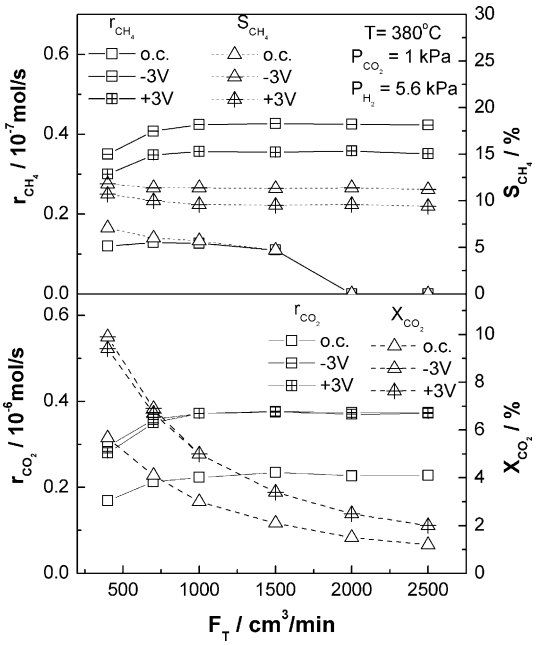

Fig. 6. Effect of the total gas flowrate on the CO_2 reduction rate, on the CO_2 conversion, on the CH_4 formation rate and on the selectivity to CH_4 under open-circuit state and anodic (+3 V) and cathodic (−3 V) polarization conditions at 380 °C utilizing 22 Rh/YSZ/Pt cells.

3.2. CO_2 hydrogenation over 20 Cu/TiO_2/YSZ/Au elements

When utilizing the 20 Cu/TiO_2/YSZ/Au cells, CH_4, C_2H_4 and CO were formed under open-circuit and under anodic and cathodic polarization conditions. This result is in agreement with previous studies at atmospheric pressure [1,3,37]. However, most literature studies over Cu-based catalysts have been performed under high pressure, i.e. 5–100 atm, where CH_3OH production becomes dominant [20–24]. It should be noted that in the aqueous electrochemical literature [60], Cu is known to be the only efficient electrocatalyst for CO_2 reduction to hydrocarbons and oxygenates at low temperatures [60] and this provides a first explanation for the observed better performance of Cu vs Rh in the present investigation.

Fig. 7 shows the steady state effect of temperature on the catalytic rate and TOF of the CO_2 reduction and on the conversion of CO_2 under open-circuit state and anodic (+3 V) and cathodic (−3 V) polarization conditions at temperatures from 220 to 380 °C and 1000 cm^3/min total gas flow rate. Under open-circuit conditions, the CO_2 conversion increases from 0.6% at 220 °C to 16% at 380 °C. Cathodic polarization leads to a significant increase in the CO_2 conversion which reaches ∼40% at 380 °C with a ρ_{CO_2} value of 2.4. Under anodic (+3 V) polarization, the maximum CO_2 conversion is 30%, with $\rho_{CO_2} = 1.8$.

Fig. 8 shows the steady state effect of temperature on the selectivity to C_2H_4, CH_4 and CO under open-circuit state and anodic (+3 V) and cathodic (−3 V) polarization conditions. Under open-circuit conditions the selectivity to C_2H_4 exhibits a maximum (∼2%) around 280 °C and the selectivity to CH_4 exhibits a maximum (∼75%) around 340 °C with a concomitant minimum in the selectivity to CO (∼22%). Anodic and cathodic polarization causes a pronounced increase in the selectivity to C_2H_4 which reaches ∼5% at 280 °C under positive polarization. The effect of potential on the selectivity to CH_4 is more complex. Below 300 °C the selectivity to CH_4 increases upon positive and negative polarization while at higher temperatures it decreases. On the other hand, CO selectivity decreases upon potential application for temperatures below 300 °C and increases at higher temperature. These maxima in hydrocarbon selectivity can be rationalized by accounting for thermal decomposition at higher temperatures.

Fig. 9 shows the steady state effect of temperature on the yield of C_2H_4, CH_4 and CO formation under open-circuit state and anodic and cathodic polarization conditions. The figure demonstrates the significant effect of polarization on product yield.

Fig. 10 shows the steady state effect of temperature on the rate enhancement ratio, ρ, and on the apparent Faradaic efficiency, Λ, for C_2H_4, CH_4 and CO upon anodic (+3 V) and cathodic (−3 V) polarization. The rate enhancement ratio for C_2H_4, $\rho_{C_2H_4}$ increases monotonically from 1.5 at 220 °C to 20 at 380 °C, while ρ_{CH_4} exhibits a maximum (∼6.5) at 280 °C. On the other hand, ρ_{CO} is maximized (∼7.5) at higher temperatures (340 °C) under negative potential application. The apparent Faradaic efficiency, Λ, is of the order of 0.02 for C_2H_4 and 0.2 for CH_4 and CO formation. These values are roughly a factor of 100 smaller than those predicted from the approximate expression $|\Lambda| \approx 2Fr_o/I_o$, valid for oxidation reactions, where r_o is the open-circuit rate (10^{-6} mol/s in the present case) and I_o is the exchange current (10^{-2} A in the present case). This large difference most likely manifests the short lifetime of the promoting O^{2-} species on the catalyst surface, as a result of the strongly reducing environment.

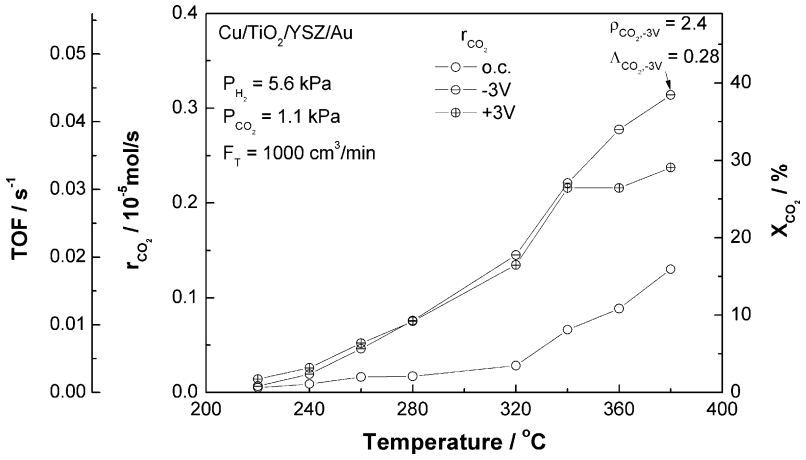

Fig. 7. Effect of temperature on the CO_2 reduction rate and TOF and on the conversion of CO_2 under open-circuit and anodic (+3 V) and cathodic (−3 V) polarization conditions utilizing 20 Cu/TiO_2/YSZ/Pt cells.

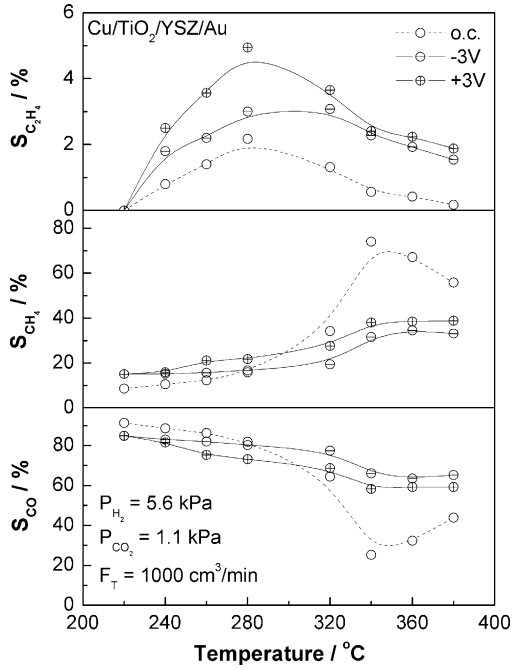

Fig. 8. Effect of temperature on the selectivity to C_2H_4, CH_4 and CO under open-circuit state and anodic (+3 V) and cathodic (−3 V) polarization conditions utilizing 20 Cu/TiO_2/YSZ/Pt cells.

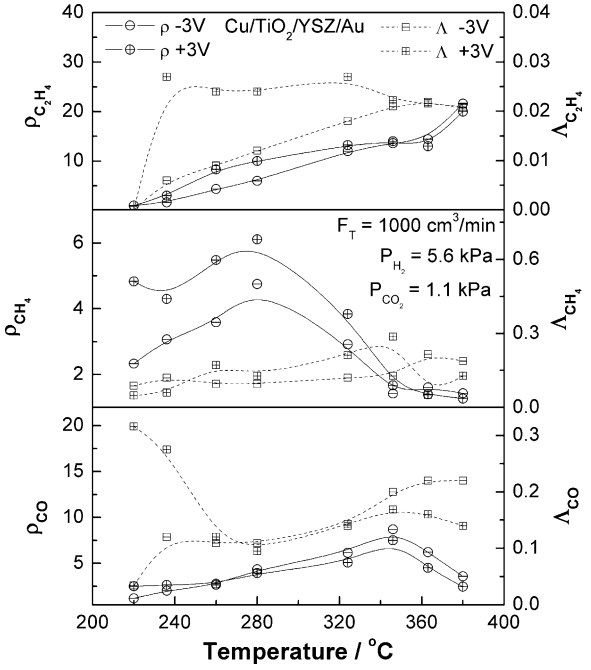

Fig. 10. Effect of temperature on the rate enhancement ratio, ρ, and on the Faradaic efficiency, Λ, of the C_2H_4, CH_4 and CO formation reactions under anodic (+3 V) and cathodic (+3 V) polarization utilizing 20 Cu/TiO_2/YSZ/Pt cells.

3.3. The promoting role of CH_3OH for CO_2 hydrogenation to CH_4

The addition of small amounts of methanol in the feed was found to have a dramatic effect on the rate and selectivity of CH_4 formation as shown in Fig. 11. The idea of adding CH_3OH in the feed is conceptually similar to the recently found strong promotional effect of adding 2-propanol [25] and 2-butanol [26] to the feed of methanol synthesis Cu/ZnO catalysts [25,26]. Thus as shown in Fig. 11, methanol addition causes a 120 °C decrease in the temperature where r_{CH4} becomes measurable and a dramatic increase in the selectivity to CH_4 from <40% without CH_3OH to 100% in presence of CH_3OH. It appears that CH_3OH adsorption blocks effectively the surface sites catalyzing the RWGS reaction (1) and at the same time forms adsorbed intermediates favoring the synthesis reaction (2).

In order to investigate this spectacular promotional effect quantitatively one must account for the fact that some CH_4 is also produced from CH_3OH, and thus we have performed a separate set of experiments feeding only CH_3OH to the reactor at the same

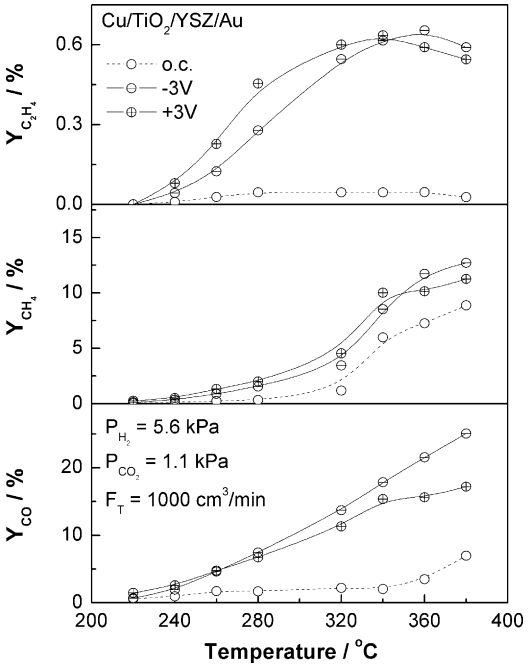

Fig. 9. Effect of temperature on the yield to C_2H_4, CH_4 and CO formation under open-circuit state and anodic and cathodic polarization condition utilizing 20 Cu/TiO_2/YSZ/Pt cells.

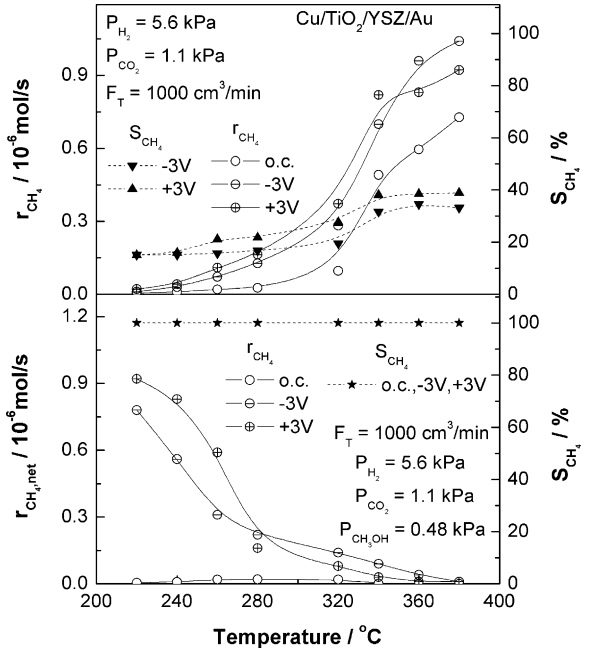

Fig. 11. Effect of temperature on the CH_4 formation rate and on the selectivity to CH_4 in absence (top) and presence (bottom) of CH_3OH in the feed under open-circuit state and anodic (+3 V) and cathodic (−3 V) polarization conditions. Feed conditions: 5.6 kPa H_2 and 1.1 kPa CO_2 (top) 5.6 kPa H_2 and 1.1 kPa CO_2 and 0.48 kPa CH_3OH (bottom); 20 Cu/TiO_2/YSZ/Au cells.

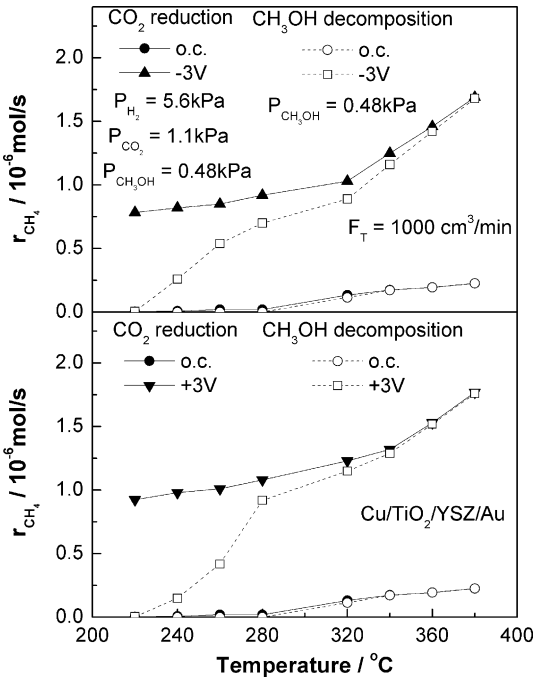

Fig. 12. Effect of temperature on the CH_4 formation reaction rate when feeding CO_2, H_2 and CH_3OH or only CH_3OH to the reactor under open-circuit state and positive (+3 V) and negative (−3 V) potential application utilizing 20 $Cu/TiO_2/YSZ/Au$ cells.

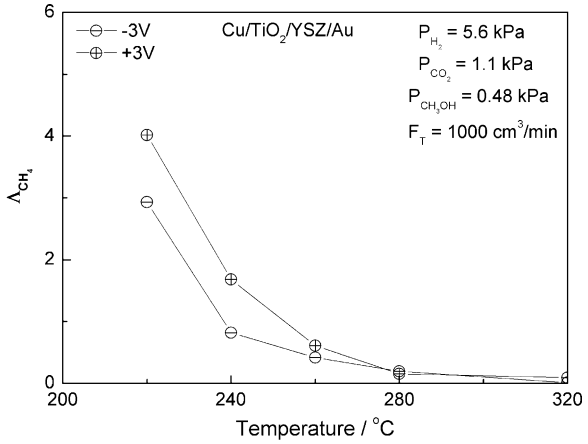

Fig. 13. Effect of temperature on the Faradaic efficiency, Λ, of the CO_2 reduction and CH_4 formation. Feed conditions: 1.1 kPa CO_2 and 0.48 kPa CH_3OH utilizing 20 $Cu/TiO_2/YSZ/Au$ cells.

concentration and temperature and measuring $r^o_{CH_4}$. We have thus computed the net increase in CH_4 production rate from

$$r_{CH_4,net} = r_{CH_4} - r^o_{CH_4} \quad (8)$$

and this is the quantity plotted in the bottom part of Fig. 11.

The corresponding values of r_{CH_4} and $r^o_{CH_4}$ are shown in Fig. 12 (filled and open symbols, respectively). One observes that the electropromoted value of r_{CH_4} at 220 °C is already 0.8×10^{-6} mol/s, higher than r_{CH_4} at 380 °C in absence of CH_3OH (0.75×10^{-6} mol/s, Fig. 11, top) and that the open-circuit $r^o_{CH_4}$ is quite low up to 380 °C (Fig. 12). However, both positive and negative polarization leads to a pronounced increase in $r^o_{CH_4}$ (Fig. 12) so that above 320 °C the rate $r^o_{CH_4}$ approaches very close to r_{CH_4} and thus $r_{CH_4,net}$ decreases significantly (Fig. 12). The main practical features are that, as already discussed, the addition of CH_3OH causes the selectivity of the CO_2 hydrogenation to CH_4 to remain near 100% over the entire temperature range 220–380 °C (Fig. 11) and also that the positively or negatively electropromoted rate of CH_4 formation also remains quite high over the same temperature range (filled symbols, Fig. 12).

Fig. 13 shows the steady state effect of temperature on the apparent Faradaic efficiency, Λ_{CH_4}, of CH_4 production, calculated from the net CH_4 formation rate, under positive (+3 V) and negative (−3 V) potential application. One observes that at 220 °C Λ_{CH_4} reaches values of 4 and 3 respectively upon positive and negative polarization.

4. Conclusions

The hydrogenation of CO_2 on Rh/YSZ catalyst-electrode films at temperatures 320–380 °C leads to CO and CH_4 formation and is affected significantly by the applied potential. The Faradaic efficiencies are small (<1) but the rate enhancement ratios ρ are pronounced (up to 5) and the change in product selectivity is significant, although the selectivity to CH_4 remains below 12%.

The same reaction on $Cu/TiO_2/YSZ$ catalyst-electrodes leads to CO, CH_4 and C_2H_4 formation. The conversion of CO_2 reaches 5% at 380 °C with ~12% selectivity to CH_4. Using the 20 $Cu/TiO_2/YSZ/Au$ cells C_2H_4, CH_4, and CO were produced under normal catalytic and polarization conditions. Under cathodic polarization (−3 V) at 380 °C the conversion of CO_2 reaches 40%, enhanced by 140%. Also, the selectivity to CH_4 and C_2H_4 was found to be ~40% with corresponding total hydrocarbon yield of 13%.

The effect of co-feeding small amounts (~0.5 kPa) of CH_3OH on the reaction rate and selectivity is very pronounced. It leads to 100% CH_4 selectivity at temperatures 220–380 °C with CO_2 conversion as high as 11% at temperatures as low as 220 °C. Under these conditions the Faradaic efficiency reaches values up to four. The results show the possibility of direct CO_2 hydrogenation to valuable products at atmospheric pressure in monolithic electropromoted reactors.

Acknowledgements

We thank the EU for partial financial support via the ELCAT project FP6-2003-NEST-A/2400 and our reviewers for helpful suggestions.

References

[1] F. Nozaki, T. Sodesawa, S. Satoh, K. Kimura, J. Catal. 104 (1987) 339.
[2] F. Solymosi, M. Pasztor, J. Catal. 104 (1987) 312–322.
[3] A.L. Lapidus, N.A. Gaidai, N.V. Nekrasov, L.A. Tishkova, Y.A. aganov, T.N. Myshenkova, Pet. Chem. 47 (2) (2007) 75–82.
[4] Y. Borodko, G.A. Somorjai, Appl. Catal. A: Gen. 186 (1999) 355–362.
[5] H. Kusama, K.K. Bando, K. Okabe, H. Arakawa, Appl. Catal. A 197 (2000) 255–268.
[6] D. Gasser, A. Baiker, Appl. Catal. 48 (1989) 279–294.
[7] Y. Amenomiya, Appl. Catal. 30 (1987) 57–68.
[8] M. Sahibzada, D. Chadwick, I.S. Metcalfe, Catal. Today 29 (1996) 367–372.
[9] M. Kishida, K. Umakoshi, J. Ishiyama, H. Nagata, K. Wakabayashi, Catal. Today 29 (1996) 335–359.
[10] M.C. Roman-Martinez, D.C. Amoros, A.L. Solano, C.S.M. de Lecea, Appl. Catal. A: Gen. 134 (1996) 159–167.
[11] F. Solymosi, A. Erdohelyi, T. Bansagi, J. Catal. 68 (1981) 371–382.
[12] Z. Zhang, A. Kladi, X.E. Verykios, J. Catal. 148 (1994) 737–747.
[13] C. Schild, A. Wokaun, A. Baker, J. Mol. Catal. 63 (1990) 243–254.
[14] M.A. Vannice, J. Catal. 37 (1975) 449–461.
[15] R.A. Koeppel, A. Baiker, A. Nokaum, Appl. Catal. A: Gen. 84 (1994) 77–102.
[16] M. Araki, V. Ponec, J. Catal. 44 (1976) 439–448.
[17] P. Panagiotopoulou, D.I. Kontarides, X.E. Verykios, Appl. Catal. A 344 (2008) 45–54.
[18] M.A. Henderson, S.D. Worley, J. Phys. Chem. 89 (1985) 1417–1423.
[19] F. Solymosi, I. Tombacz, J. Koszta, J. Catal. 95 (1985) 578–586.
[20] J.A. Brown Bourzutschky, N. Holms, A.T. Bell, J. Catal. 124 (1990) 73–85.
[21] K.G. Chanchlani, R.R. Hudgins, P.L. Silveston, J. Catal. 136 (1992) 59–75.
[22] Y. Nitta, O. Suwata, Y. Okamoto, T. Imanaka, Catal. Lett. 26 (1994) 345–354.
[23] P.C.K. Vesborg, I. Chorkendorff, I. Knudsen, O. Balmes, J. Nerlov, A.M. Molenbroek, B. Clause, S. Helveg, J. Catal. 262 (2009) 65–72.

[24] F. Arena, G. Italiano, K. Barbera, S. Bordiga, G. Bonura, L. Spadaro, F. Frusteri, Appl. Catal. A: Gen. 350 (2008) 16–23.
[25] R. Yang, Y. Zhang, N. Tsubaki, Catal. Commun. 6 (2005) 275–279.
[26] P. Reubroycharoen, T. Vitidsant, Y. Yoneyama, N. Tsubaki, Catal Today 89 (2004) 447–454.
[27] Y. Hori, H. Wakebe, T. Tsukamoto, O. Koga, Surf. Sci. 335 (1995) 258–263.
[28] H. Ando, Q. Xu, M. Fujiwara, Y. Matsumura, M. Tanaka, Y. Souma, Catal. Today 45 (1998) 229–234.
[29] A. Trovarelli, C. Mustazza, G. Dolcetti, Appl. Catal. 65 (1990) 129.
[30] M. Marwood, R. Doepper, A. Renken, Appl. Catal. A: Gen. 151 (1997) 223–246.
[31] J.L. Falconer, A.E. Zagli, J. Catal. 62 (1980) 280–285.
[32] G.D. Weatherbee, C.H. Bartholomew, J. Catal. 77 (1982) 460–472.
[33] S. Fujita, H. Terunuma, H. Kobayashi, N. Takezawa, React. Kinet. Catal. Lett. 33 (1) (1897) 179–184.
[34] P. Biloen, J.N. Helle, F.G.A. Van Berg, W.M.H. Sachtler, J. Catal. 81 (1983) 450–463.
[35] R.A. Fiato, E. Iglesia, G.W. Rice, S.L. Iron, Stud. Surf. Sci. Catal. 114 (1998) 339.
[36] J.W.E. Coenen, P.F.M.T. Van Nisselrooy, M.H.J.M. De Croon, P.F.H.A. van Dooren, R.Z.C. Van Meertrn, Appl. Catal. 25 (1986) 1–8.
[37] V.M. Vlassenko, G.E. Yuzefovich, Russ. Chem. Rev. 38 (1969) 9.
[38] M.C. Roman-Martinez, D. Cazola-Amoros, A. Linares-Solano, C. Salinas-Martinez de Lecea, Appl. Catal. A: Gen. 134 (1996) 159–167.
[39] C.G. Vayenas, S. Bebelis, S. Ladas, Nature 343 (1990) 625.
[40] C.G. Vayenas, K. Koutsodontis, J. Chem. Phys. 128 (2008) 182506.
[41] C.G. Vayenas, S. Bebelis, C. Pliangos, S. Brosda, D. Tsiplakides, Electrochemical Activation of Catalysis: Promotion, Electrochemical Promotion and Metal-Support Interactions, Kluwer Academic/Plenum Publishers, New York, 2001.
[42] N.A. Anastasijevic, H. Baltruschat, J. Heitbaum, Electrochim. Acta 38 (1993) 1067.
[43] Ch. Kokkofitis, G. Karagiannakis, S. Zisekas, M. Stoukides, J. Catal. 234 (2005) 476.
[44] N. Kotsionopoulos, S. Bebelis, J. Appl. Electrochem. 35 (2005) 1253.
[45] S. Neophytides, D. Tsiplakides, P. Stonehart, M. Jaksic, C.G. Vayenas, Nature (London) 370 (1994) 292.
[46] I.M. Petrushina, V.A. Bandur, F. Cappeln, N.J. Bjerrum, J. Electrochem. Soc. 147 (2000) 3010.
[47] C. Cavalca, G. Larsen, C.G. Vayenas, G. Haller, J. Phys. Chem. 97 (1993) 6115.
[49] G. Pacchioni, F. Illas, S. Neophytides, C.G. Vayenas, J. Phys. Chem. 100 (1996) 16653.
[50] I. Riess, C.G. Vayenas, Solid State Ionics 159 (2003) 313.
[51] A. Jaccoud, C. Falgairette, G. Foti, Ch. Comninellis, Electrochim. Acta 52 (2007) 7927.
[52] A. de Lucas-Consuegra, F. Dorado, C. Jimenez-Borja, J.L. Valverde, J. Appl. Electrochem. 38 (2008) 1151.
[53] S. Bebelis, H. Karasali, C.G. Vayenas, J. Appl. Electrochem. 38 (2008) 1127.
[54] S. Bebelis, H. Karasali, C.G. Vayenas, Solid State Ionics 179 (2008) 1391.
[55] S.P. Balomenou, D. Tsiplakides, A. Katsaounis, S. Thiemann-Handler, B. Cramer, G. Foti, Ch. Comninellis, C.G. Vayenas, Appl. Catal. B 52 (2004) 181.
[56] S. Souentie, A. Hammad, S. Brosda, G. Foti, C.G. Vayenas, J. Appl. Electrochem. 38 (2008) 1159–1170.
[57] E.A. Baranova, G. Foti, H. Jotterand, Ch. Comninellis, Top. Catal. 44 (3) (2007) 355.
[58] E.A. Baranova, A. Thursfield, S. Brosda, G. Foti, Ch. Comninellis, C.G. Vayenas, J. Electrochem. Soc. 152 (2) (2005) E40.
[59] C. Pliangos, I.V. Yentekakis, S. Ladas, C.G. Vayenas, J. Catal. 159 (1996) 189.
[60] Y. Hori, Electrochemical CO_2 reduction on metal electrodes, in: C.G. Vayenas, R.E. White, M.E. Gamboa-Aldeco (Eds.), Modern Aspects of Electrochemistry, 42, Springer, New York, 2008 , p. 89 (Chapter 3).